Adenine−Uridine Base Pairing at the Water−Solid-Interface

Michael Weisser, Josua Käshammer, Bernhard Menges, Jin Matsumoto,† Fumio Nakamura,† Kuniharu Ijiro,† Masatsugu Shimomura,† and Silvia Mittler*

Contribution from the Max-Planck-Institut für Polymerforschung, Ackermann Weg 10, 55128 Mainz, Germany, and Research Institute for Electronic Science, Hokkaido University, N12W6, Sapporo 060, Japan

Received February 11, 1999. Revised Manuscript Received August 24, 1999

Abstract: The formation of the base pair adenine-uracil at a water−solid interface, at an immobilized monolayer of adenine disulfide with adenine groups exposed to the very surface, respectively, is shown here. To overcome the steric hindrance of tightly packed adenine groups in a pure adenine thiolate monolayer on gold, the formation of self-assembled monolayers out of a binary mixture of the adenine disulfide and CH_3- or OH-terminated thiols are investigated. Electro-chemical investigations, surface plasmon spectroscopy (PSP, plasmon surface polariton), multimode waveguide-PSP-coupling spectroscopy, contact angle measurements, and spontaneous desorption time-of-flight mass spectrometry were used to characterize the monolayers. The specific base pairing was investigated for a variety of monolayer compositions. A specific base pairing was successful for an optimized mixed adenine/OH-terminated thiol monolayer. Nevertheless unspecific binding is a problem.

Introduction

To tailor molecular organization is one of the final goals of supra molecular chemistry[1,2] and is essential for the design of molecular devices.[3,4] Weak intermolecular interactions such as hydrogen bonds,[5] as well as the interactions in typical guest−host systems such as in the biotin-streptavidin-system[6,7] or in the family of the cyclic molecules such as cylodextrins[8−12] or calixarenes[13,14] are well-known architectural tools for the assembling of molecular organization. Nature has used these tools in a wide variety to create functionality.[15] Cell−cell recognition or communication via guest−host reactions of proteins or the most versatile DNA double helix are typical examples where molecular organization based on specific intermolecular interactions delivers a very particular biological functionality and therefore contains well-defined information.[15]

Hydrogen bonding was studied intensely for the past decades within three-dimensional geometry, for example, DNA in solution.[15] Two-dimensional arrangements of molecules being able to develop hydrogen bonds with a fitting partner were studied for the first time by Kurihara et al. in 1991.[16] The two-dimensional geometry was achieved by an air−water interface on a Langmuir−Blodgett (LB) trough, where the hydrogen bonding took place in the water phase. An amphiphilic diaminotriazine was able to selectively bind nucleosides and nucleic acid bases. In 1997 the base pairing of cytosine with guanosine at the air−water interface was found as the first two-dimensional system being biologically relevant.[17] In the same year Matsuura et al.[18] have demonstrated the two-dimensional hydrogen bonding on a solid−air interface via a self-assembled monolayer. Recently an artificial hydrogen bonding molecular pair was demonstrated at a solid−hydrophilic organic solvent interface.[19] Here we like to demonstrate the possibility of using hydrogen bonding in a two-dimensional array at the solid−water interface. Hydrogen bonding in water is especially significant due to its relevance to biological molecular recognition. The base pair adenine-uracil was chosen. Therefore a disulfide with two spacers and an adenine headgroup at each end (Figure 2) was synthesized for forming self-assembled adenine thiolate monolayers exposing adenine groups to the very surface of a solid metal substrate.[20] Uridine as the water soluble derivative of uracil was investigated for the binding processes. For unspecific binding tests cytidine was used. Figure 1 demonstrates the specific recognition and binding via hydrogen bonds of the base pairs adenine/uracil and guanine/cytosine. The chemical structures of the water soluble uridine and cytidine used in this study are shown as well (Figure 1b).

* Corresponding author: e-mail: mittler@mpip-mainz.mpg.de.
† Hokkaido University.

(1) Lehn, J. M. *Angew. Chem., Int. Ed. Engl.* **1989**, *27*, 89.
(2) Lehn, J. M. *Angew. Chem., Int. Ed. Engl.* **1990**, *29*, 1304.
(3) Ringsdorf, H.; Schlarb, B.; Venzmer, J. *Angew. Chem., Int. Ed. Engl.* **1989**, *27*, 113.
(4) Kunitake, T. *Angew. Chem., Int. Ed. Engl.* **1992**, *31*, 706.
(5) Boschke, F. L., Ed. Hydrogen bonds. In *Topics in Current Chemistry*; Springer-Verlag: Heidelberg, 1984; Vol. 120.
(6) Spinke, J.; Liley, M.; Schmitt, F.-J.; Guder, H.-J.; Angermaier, L.; Knoll, W. *J. Chem. Phys.* **1993**, *99*, 7012.
(7) Spinke, J.; Liley, M.; Guder, H.-J.; Angermaier, L.; Knoll, W. *Langmuir* **1993**, *9*, 1821.
(8) Saenger, W. *Angew. Chem., Int. Ed. Engl.* **1980**, *19*, 344.
(9) Wenz, G. *Angew. Chem., Int. Ed. Engl.* **1994**, *33*, 803.
(10) Nelles, G.; Weisser, M.; Back, R.; Wohlfart, P.; Wenz, G.; Mittler-Neher, S. *J. Am. Chem. Soc.* **1996**, *118*, 5039.
(11) Weisser, M.; Nelles, G.; Wohlfart, P.; Wenz, G.; Mittler-Neher, S. *J. Phys. Chem.* **1996**, *100*, 17893.
(12) Weisser, M.; Nelles, G.; Wenz, G.; Mittler-Neher, S. *Sens. Actuators, B* **1997**, *38−39*, 58.
(13) Böhmer, V. *Angew. Chem., Int. Ed. Engl.* **1995**, *34*, 713.
(14) Huisman, B.-H.; Kooymann, R. P. H.; van Veggel, F. C. J. M.; Reinhoudt, D. N. *Adv. Mater.* **1996**, *8*, 561.
(15) Hoppe, W.; Lohmann, W.; Markl, H.; Ziegler, H. *Biophysik*; Springer-Verlag: Heidelberg, 1982.
(16) Kurihara, K.; Ohto, K.; Honda, Y.; Kunitake, T. *J. Am. Chem. Soc.* **1991**, *113*, 5077.
(17) Shimomura, M.; Nakamura, F.; Ijiro, K.; Taketsuna, H.; Tanaka, M.; Nakamura, H.; Hasebe, K. *J. Am. Chem. Soc.* **1997**, *119*, 2341.
(18) Matsuura, K.; Ebara, Y.; Okahata, Y. *Langmuir* **1997**, *13*, 814.
(19) Motesharei, K.; Myles, D. C. *J. Am. Chem. Soc.* **1998**, *120*, 7328.
(20) Ulman, A. *Chem. Rev.* **1996**, *96*, 1533.

10.1021/ja990447b CCC: $19.00
Published on Web 12/18/1999

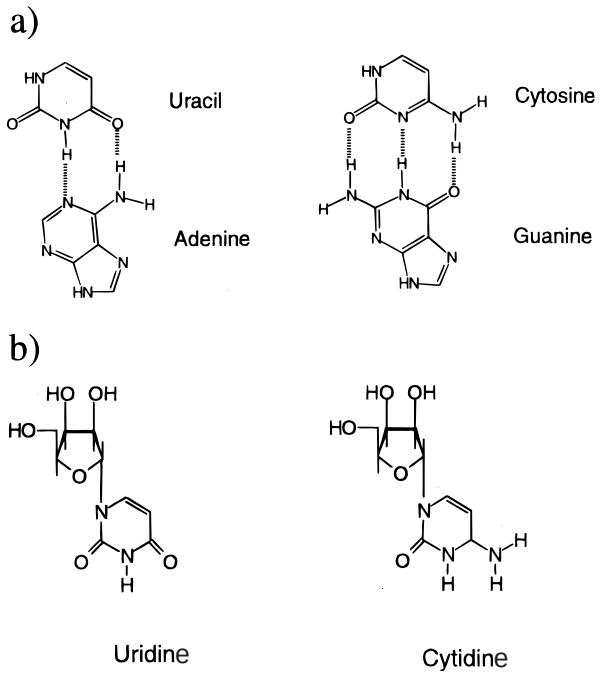

Figure 1. (a) Specific recognition and binding of the base pairs adenine/uracil and guanine/cytosine. (b) Chemical structure of uridine and cytidine.

Materials

11-mercapto-1-undecanol ($OH(CH_2)_{11}SH$, Aldrich, OHT) and decane thiol ($CH_3(CH_2)_9SH$, Aldrich, CH_3T) (Figure 2) were used without further purification.

Synthesis of 11-[2-(9-Adeninyl)propionyloxy]undecyl Disulfide (A). Nuclear magnetic resonance (NMR) spectra were recorded with a JEOL EX-400 spectrometer (^1H, 400 MHz). Chemical shifts are reported in parts per million (ppm) downfield of tetramethylsilane (TMS). Fast atom bombardment (FAB) mass spectra were recorded with a JEOL HX110 mass spectrometer with a cesium ion source and positive ion detection. Fourier transform infrared (FTIR) spectra were recorded with a JASCO FTIR-300 spectrometer. The samples were prepared as KBr pellets.

Pyridine was freshly distilled from CaH_2. Dimethylformamide (DMF) was freshly distilled. All other reagents were of the highest available commercial quality and used without further purification.

Ethyl 3-(9-Adeninyl)propionate (1).[21,22] A mixture of adenine (10 g, 74 mmol), metal sodium (74 mg, 32 mmol), and ethyl acrylate (24 mL, 0.22 mol) in 200 mL of anhydrous ethanol was refluxed for 2 h. The precipitate was collected and recrystallized in ethanol to give ethyl 3-(9-adeninyl)propionate (1) in 77% yield: mp 170−171 °C; ^1H NMR ($CDCl_3$) d 1.20−1.23 (t, $J = 7.2$ Hz, 3 H), 2.91−2.93 (t, $J = 3.2$ Hz, 2 H), 4.11−4.16 (q, $J = 7.6$ Hz, 2 H), 4.47−4.51 (t, $J = 6.4$ Hz, 2 H), 5.49 (s, 2 H), 7.87 (s, 1 H), 8.35 (s, 1 H); IR 1720, 1680, 1609, 1205, 651 cm^{-1}.

3-(9-Adeninyl)propionic Acid (2). The ester (**1**) (13 g, 55 mmol) in 250 mL of 5 N HCl was refluxed for 3 h. Neutralization of the hydrochloride salt of (**2**) by sodium carbonate solution gave 3-(9-adeninyl)propionic acid (2) in 67% yield: mp 285−288 °C; ^1H NMR (DMSO-*d*) d 2.84−2.87 (t, $J = 7.2$ Hz, 2 H), 4.33−4.36 (t, $J = 6.8$ Hz, 2 H), 6.96 (s, 2 H), 8.04 (s, 1 H), 8.13 (s, 1 H); IR 1703, 1617, 1410, 645 cm^{-1}.

4-Nitrophenyl 3-(9-Adeninyl)propionate (3). *p*-Nitrophenyl trifluoroacetate (7.1 g, 30 mmol) was added to a suspension of 3-(9-adeninyl)propionic acid (2) (5.0 g, 24 mmol) in 150 mL of dry pyridine. The mixture was stirred for 2 days at 25 °C to give a clear solution. After vacuum distillation of pyridine at 60 °C to complete dryness the residual solid was washed with benzene while stirring. The fine white product was filtered and washed with benzene to give *p*-nitrophenyl ester (**3**) in 75% yield. The product was immediately used for a next reaction without further purification.

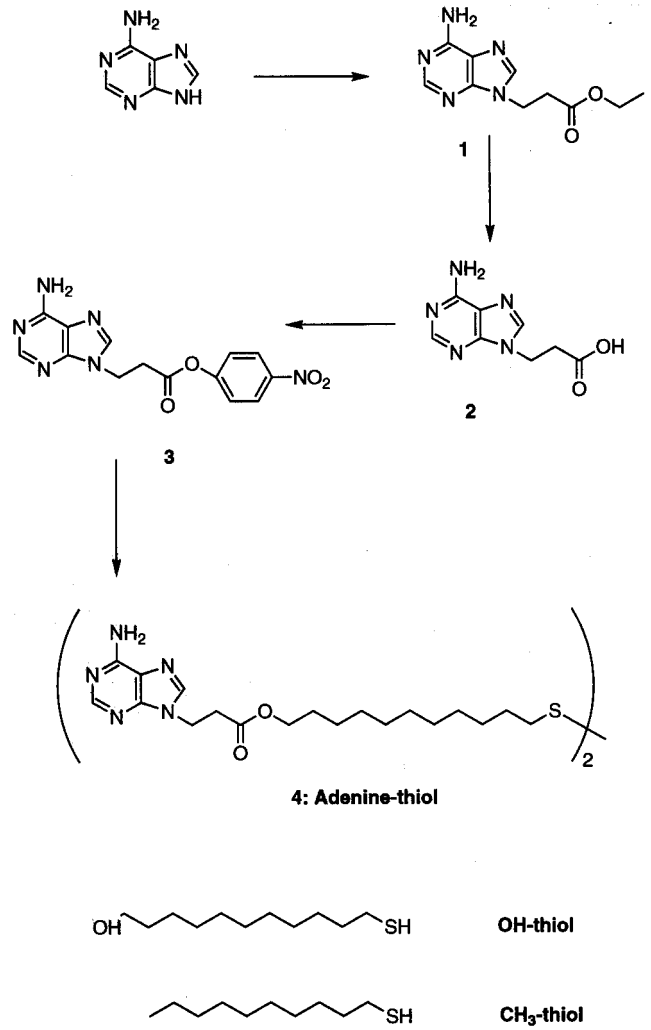

Figure 2. Synthesis scheme for 11-[2-(9-adeninyl)propionyloxy]-undecyl disulfide and the structure formula of the OHT and the CH_3T.

11-[2-(9-Adeninyl)propionyloxy]undecyl Disulfide (4). A mixture of *p*-nitrophenyl ester (1.0 g, 2.7 mmol), imidazol (0.44 g, 6.4 mmol) and 11-mercapto-1-undecanol (0.68 g, 3.2 mmol) in a mixture of 10 mL of *N,N*-dimethylformamide (DMF) and 10 mL of dichloromethane was stirred for 2 days at 25 °C. The precipitate was collected and washed with dichloromethane, ethanol, water, and ethanol. The product was recrystallized in ethanol to give 11-[2-(9-adeninyl)propionyloxy]-undecyl disulfide (**4**) as a mixture with a thioester compound as a side product, 11-[2-(9-adeninyl)propionylthio]-1-undecanol (50 wt %) (13% yield). The product was used without further purification due to a difficulty of further separation and considerably small probability of the thioester binding to the gold surface: mp 153−155 °C; ^1H NMR (DMSO-*d*) d 1.21−1.23 (m, 28 H), 1.37−1.46 (m, 8 H), 2.67−2.70 (t, $J = 7.6$ Hz, 4 H), 2.78−2.82 (t, $J = 7.6$ Hz, 4 H), 3.96−3.99 (t, $J = 6.4$ Hz, 4 H), 4.39−4.42 (t, $J = 7.2$ Hz, 4 H), 6.99 (s, 4 H), 8.05 (s, 2H), 8.14 (s, 2H); IR 2919, 2850, 1727, 1645, 1594, 1199 cm^{-1}; MS 786 (M^+).

The synthesis scheme for 11-[2-(9-Adeninyl)propionyloxy]undecyl disulfide is shown in Figure 2. The materials were dissolved in ethanol (Chromasolv, Riedel-de-Haen).

Experimental Setup

(A) Immobilization of the Adenine. The self-assembled monolayers were formed on gold films, vacuum-evaporated at a pressure of $5 \cdot 10^{-6}$ mbar onto cleaned LaSFN9 (Schott) substrates. After preparation, the

(21) Lira, E. P.; Huffman, C. W. *J. Org. Chem.* **1966**, *31*, 2188.
(22) Overberger, C. G.; Inaki, Y. *J. Polym. Sci., Polym. Chem. Ed.* **1979**, *17*, 1739.

gold-coated substrates were allowed to cool under vacuum for approximately 30 min and were then immediately placed in solution of the appropriate self-assembling adenine disulfide/alkylthiol binary mixture or stored under argon. All adsorption processes were performed in ethanol (Chromasolve, Riedel-de-Haen) with a concentration of 0.5 mM. The mole fraction of the adenine in the OH- or CH_3-terminated thiol was varied from 0 to 1 by mixing corresponding volumina taking the side product of the thioester into account. The uridine as the binding base to adenine and cytidine for testing of unspecific binding were solved in milli-Q water (Millipore) as 0.5 mM solutions.

The preparation of the waveguide surface plasmon (PSP, plasmon surface polariton)-coupling device is described elsewhere.[23]

(B) Electrochemical Measurements. Electrochemistry was performed on a NIKKO KEISOKU NPGFZ-2501-A potentio-galvanostat. Working electrodes were typically 1 cm^2 evaporated gold (2000 Å) on tin−indium-oxide (ITO) glass. Monolayers of OHT and adenine thiolate[20] were prepared on the electrodes in the same manner as that described above. A platinum wire was used as a counter electrode. A saturated calomel electrode (SCE) was used as reference in all electrochemical experiments. The potential was initiated at 0.00 V and cycled at 50 mV/s between −1.45 and 0.00 V in 0.5 M aqueous KOH solution. Deionized water, which was purified by passage through a milli-Q filtration system, was used for all solution preparation. Solutions were degassed with N_2 for 15 min prior to the measurements.

(C) Surface Plasmon Spectroscopy (PSP, Plasmon Surface Polariton). PSP measurements were performed to study the optical film thickness of the SAM with respect to the concentration of the adenine in the binary mixture of the self-assembly solution. Here the Kretschmann configuration[24] was used with a 50 nm gold film evaporated onto a substrate, which is then optically matched to the base of a 90° LaSFN9 glass prism (n =1.85 at λ = 632.8 nm). Thus, the plasmon surface polaritons are excited at the metal/dielectric interface, upon total internal reflection of the laser beam (HeNe, λ = 632.8 nm, power 5 mW) at the prism base. By varying the angles of incidence of the laser beam, a plot of reflected intensity as a function of the angle of incidence is obtained. The reflected intensity shows a sharp minimum at the PSP resonance angle which depends on the precise architecture of the metal/dielectric interface and is defined by the matching condition for energy and momentum between the evanescent photons and the plasmon surface polariton. Adsorption processes occurring at the gold interface were followed in real time by selecting an appropriate angle of incidence and monitoring the reflected intensity as a function of time. Knowledge of the form of the resonance curve allows this intensity to be interpreted as a shift in the angle of resonance.

From a Fresnel simulations to the resonance curve for bare gold surfaces, it is possible to obtain the dielectric constant and the thickness of the gold layer. Addition of a thin layer to the surface of the gold typically shifts the position of the resonance to a higher angle, and a simulation of this second resonance curve determines the optical thickness, (nd), of the layer. Although plasmon surface polariton measurements allow the determination of an average optical thickness of an adsorbed film, accurate conversion of this optical thickness to a geometrical thickness requires knowledge of the refractive index of the film, a parameter which depends on both the molecular composition of the film and the packing density. In practice, it is not possible to distinguish between a thin film with a high refractive index and a film twice as thick but with half the refractive index contrast in the medium. For the data analysis here a refractive index of n = 1.5 was chosen for both the adenine thiolate and the diluting thiols, OHT and CH_3T. The data for the pure adenine thiolate and the pure OHT and CH_3T monolayers were evaluated using a concentration-dependent refractive index measurement (dn/dc) of the materials in ethanol[25] and calculate the surface concentration c in [mol/cm^2].[26]

$$c = \frac{dc}{dn}\Delta n d \quad (1)$$

(D) Contact Angle Measurement. Advancing and receding contact angles of water on the films were measured using a contact angle microscope (Krüss G-1) under ambient conditions, while the volume of the drop is increased or decreased at the minimum rate required for movement of the water/air/solid triple point.

(E) Spontaneous Desorption Time-of-Flight Mass Spectrometry (SDMS). The measurements were performed using a linear time-of-flight (TOF) mass spectrometer in high vacuum at a pressure of about 1×10^{-6} mbar. The self-assembled monolayers were deposited on 50 nm thick gold films evaporated on glass slides that were covered first with a 2 nm chromium film to increase the mechanical stability. Atomar and molecular ions from the sample were released by spontaneous desorption, a secondary ion process in which the sample is not bombarded by particles from an external source.[27] Primary ions of adsorbates are field-desorbed from the edges of an acceleration grid located in front of the sample. These ions are accelerated toward the sample gaining keV energies. They finally sputter secondary ions from the sample, and these are analyzed with the TOF mass spectrometer. Spectra of negative secondary ions are recorded using the simultaneously emitted secondary electrons from the sample surface as trigger particles. An acceleration voltage of 9.5 kV was applied to the sample. The recording time of a spectrum was 20−40 min. Within one spectrum mass peaks of interest were integrated and normalized with the number of start events with one or more corresponding stop events. This leads to a relative ion yield that allows the comparison of the intensities of equivalent peaks in different spectra.

(F) Multimode waveguide-PSP-coupling. To determine the thickness and the refractive index of the SAM independently from each other the recently published method of multimode waveguide-PSP-coupling was used.[23,28−36] An ion-exchanged buried multimode glass channel waveguide was coated with a 40 nm thick gold film to enable the coupling of the waveguide modes into the surface plasmon. Due to the resonant PSP coupling the dispersion of the effective refractive index of the waveguide mode and therefore the imaginary part of the effective refractive index is altered, which leads to a change in the transmitted light intensity of the waveguide modes. This intensity change can be back-calculated via Fresnel theory to an average thickness and an average refractive index of the SAM.[23,37]

Monolayer Characterization

Measurements. To find the optimum binding conditions at the solid−water interface of the uridine the adenine thiolate is laterally diluted by the OHT or CH_3T.[6,7] Due to the bulky headgroup of the adenine disulfide, monolayers of the pure adenine thiolate might not be very ordered and the structure of the film not very well understood.[38] Therefore, the mole fraction x of the adenine within the self-assembly solutions was systematically varied from pure OHT or CH_3T solutions (x = 0) to pure adenine disulfide solutions (x = 1).

The length of the anchor groups of the adenine disulfide and the diluting thiols was chosen to achieve via van der Waals

(23) Weisser, M.; Menges, B.; Mittler-Neher, S. *Sens. Actuators, B*, in press.
(24) Kretschmann, E. *Opt. Commun.* **1972**, *6*, 185.
(25) Becker, A.; Köhler, W.; Müller, B. *Ber. Bunsen-Ges. Phys. Chem.* **1995**, *99*, 600.
(26) Miller, C. E.; Meyer, W. H.; Knoll, W.; Wegner, G. *Ber. Bunsen-Ges. Phys. Chem.* **1992**, *96*, 869.
(27) Voit, H.; Schoppmann, C.; Brandl, D. *Phys. Rev. B* **1993**, *48*, 17517.
(28) Lavers, C. R.; Wilkinson, J. S. *Sens. Actuators, B* **1994**, *22*, 75.
(29) Harris, R. D.; Wilkinson, J. S. *Sens. Actuators, B* **1995**, *29*, 261.
(30) Weiss, M. N.; Srivastava, R.; Groger, H.; Lo, P.; Luo, S.-F. *Sens. Actuators, A* **1996**, *51*, 211.
(31) Ctyroky, J.; Homola, J.; Skalsky, M. *Opt. Quantum Electron.* **1997**, *29*, 301.
(32) Mouvet, C.; Harris, R. D.; Maciag, C.; Luff, B. J.; Wilkinson, J. S.; Piehler, J.; Brecht, A.; Gauglitz, G.; Abuknesha, R.; Ismail, G. *Anal. Chim. Acta* **1997**, *338*, 109.
(33) Brecht, A.; Gauglitz, G. *Anal. Chim. Acta* **1997**, *347*, 219.
(34) Homola, J.; Ctyroky, J.; Skalky, M.; Hradilova, J.; Kolarova, P. *Sens. Actuators, B* **1997**, *38−39*, 286.
(35) Ctyroky, J.; Homola, J.; Skalsky, M. *Electron. Lett.* **1997**, *33*, 1246.
(36) Weisser, M.; Menges, B.; Mittler-Neher, S. *SPIE* **1998**, *3414*, 250.
(37) TRAMAX, University of Jena, Institut of Theoretical Optics, Max Wien Platz 1, 07743 Jena, Germany.
(38) Qian, J.; Hentschke, R.; Knoll, W. *Langmuir* **1997**, *13*, 7092.

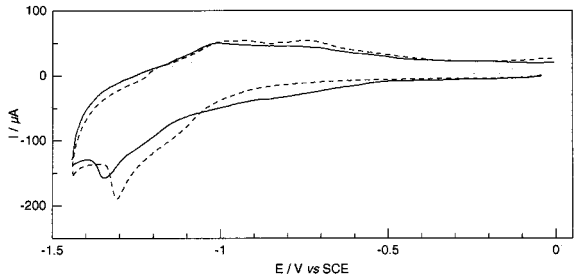

Figure 3. Cyclic voltammograms initiated at 0.00V for the reductive desorption of OHT (− − −) and adenine thiolate (—) monolayers from Au surfaces.

Table 1. Charge (Q), Surface Coverage (Γ) and Area per Molecule (A) Determined from Electrolysis of OHT and Adenine Thiolate Monolayers Assembled on Au[a]

thiolate	Q [μC/cm^2]	Γ [mol/cm^2]	A [Å^2]
OHT	73.13 ± 7.00	7.6 ± 0.7	22 ± 3
adenine	62.05 ± 6.00	6.4 ± 0.6	26 ± 3

[a] The data were not corrected for surface roughness of the gold.

interactions between these chains a well-ordered mixed monolayer.[39−41]

An electrochemical approach for determining the surface coverage of thiolate monolayers formed at gold electrodes were reported.[42,43] The approach is based on the voltammetric measurement of the charge passed for the one-electron reductive desorption of the resulting gold-bound thiolate layer (Au−SR) in alkaline solution (pH > 11): $Au{-}SR + e^- \rightarrow Au(0) + -SR$. Figure 3 shows the cyclic voltammograms (CV), the current−voltage (i−E) curves for the OHT and the adenine thiolate monolayers. The large cathodic wave with a peak current near −1.30 V and −1.35 V in the first scan of the OHT and the adenine thiolate layers, respectively, arises from the one-electron reduction. The charge associated with the electrode reaction (Q) was determined by integration of the cathodic peak in the first voltammetric scan. A surface coverage (G) and a molecular area (A) of thiolate compounds bound to the gold surfaces were calculated from the charge values and the apparent area of the electrode. Those values are summarized in Table 1. The surface coverage (Γ) both of OHT and adenine thiolate layers coincide within the experimental errors with these of alkanethiolate layers.[42] We therefore assume that the side product of the thioester is not binding to the gold.

Mass spectra were taken from SAMs which were self-assembled out of solutions with varying adenine disulfide concentration. In Figure 4 the mass spectra for the pure adenine thiolate SAM (**4a**), the pure CH_3T SAM (**4b**) and a SAM self-assembled out of a 19:2 (A/CH_3T), $x = 0.95$, binary solution (**4c**) are shown. In all spectra the gold ions Au^- (m/z = 197 u), Au_2^- (m/z = 394 u), and Au_3^- (m/z = 591 u) are found. Besides these gold signals peaks are found which appear periodically with the higher gold clusters. For example, at m/z = 221, 222, and 223 u peaks are found which belong to Au^- with pump oil contaminations of m/z = 24, 25, and 26 u.[44] The spectrum of the pure adenine thiolate monolayer shows that only fragments of the molecule are desorbed: the molecular peak of the adenine thiolate at m/z = 393 u is missing as well as fragments which would arise from the thioester. The CN^- fragment of the heterocyclic purin ring at m/z = 26 u can be seen by the inversion of the intensity of the pump oil peaks at m/z = 25 or 26 u, respectively. The deprotonated adenine (A^-) is found at m/z = 134 u. A frequent fragment of the adenine thiolate is the deprotonated carboxyethyle ($A + EtCOO^-$, m/z = 206 u). The peak at m/z = 229 u of the AuS^- fragment shows the covalent bond between the adenine compound and the gold. A series of small mass peaks arise from small fragments from the alkyl chain and the adenine. They are not discussed any beyond this point, because they are common in all the spectra under investigation and yield no further information.

The pure CH_3T monolayer shows similar low mass peaks of fragments from the alkyl chains. The lightest specific fragment is the decan thiolate ion ($S(CH_2)_9CH_3^-$) at m/z = 173 u. Stronger is the peak at m/z = 370 u, the gold decane thiolate ion ($Au + CH_3T^-$). Unusually high is the peak at m/z = 543 u, which can be ascribed to a gold didecanthiolate ion ($Au + (CH_3T)^-_2$). The fragment at m/z = 229 u is found in this spectrum as well, pointing to the covalent bond between the CH_3T and the gold surface.

The spectrum of the binary mixture shows all of the characteristic peaks of both adsorbed species.

The analogue mass spectra were taken for OHT as the diluting molecule. Figure 5 shows the mass spectrum of the pure adenine thiolate SAM (**5a**, like **3a**, for comparison shown again), the pure OHT SAM (**5b**) and of a SAM which was self-assembled out of a 19:2 (adenine/OHT), $x = 0.95$, binary solution (**5c**). In the low mass regime the spectrum of the OH terminated thiol is identical with all the other investigated monolayers. The only characteristic peak is found at m/z = 203 u, the deprotonated 11-mercapto-1-undecanol ion (OHT^-). Gold thiolate ions were not found. The AuS^- peak at m/z = 229 u is present. The mass spectrum of the monolayer of the binary mixture depicts the characteristic peaks of both adsorbed species.

For the PSP measurements monolayers out of binary mixtures between the diluting thiols and the adenine disulfide were self-assembled for 8−10 h. For the pure materials the surface density or the area per molecule, respectively was determined via the dn/dc measurement and eq 1. For the thickness determination a refractive index of 1.5 was chosen for all three materials. The results for the pure materials are summarized in Table 2. The

Table 2. Thickness, dn/dc-values and Surface Density of the Pure CH_3T, OHT, and 11-[2-(9-Adeninyl)propionyloxy]undecyl Disulfide

	CH_3T	OHT	adenine thiolate
thickness [Å] (n = 1.5)	10 ± 1.5	13 ± 1.7	28 ± 1.8
dn/dc [ml/mol]	18.4 ± 1	26.5 ± 1.2	70.3 ± 1.6
area per molecule [Å^2]	22 ± 3	24 ± 3	31 ± 3

area per molecule is similar within the errors for the two diluting thiols (22−24 Å^2), the bound adenine thiolate depicts a larger area per molecule of 31 Å^2 because of the large adenine headgroup. The thicknesses of the pure and the mixed monolayers are shown with respect to the mole fraction x of the adenine in the self-assembly solution in Figure 6. The film thickness increases very slightly from the pure OHT or CH_3T (x = 0) to x = 0.7. From 70 to 100% adenine in the self-assembly solution the film thickness increases strongly to the final adenine thiolate monolayer thickness of 28 Å. The concentration of the adenine in the monolayer is obviously different from the concentration within the self-assembling solution.

(39) Porter, M. D.; Bright, T. B.; Allara, D. L.; Chidsey, C. E. D. *J. Am. Chem. Soc.* **1987**, *109*, 3559.
(40) Hautmann, J.; Klein, M. L. *J. Chem. Phys.* **1989**, *91*, 4994.
(41) Fenter, P.; Eisenberger, P.; Liang, K. S. *Phys. Rev. Lett.* **1993**, *70*, 2447.
(42) Widrig, C. A.; Chung, C.; Porter, M. D. *J. Electroanal. Chem.* **1991**, *310*, 335.
(43) Walczak, M. M.; Popenoe, D. D.; Deinhammer, R. S.; Lamp, B. D.; Chung, C.; Porter, M. D. *Langmuir* **1991**, *7*, 2687.
(44) Wohlfart, P. Ph.D. Thesis, Mainz, Germany, 1997.

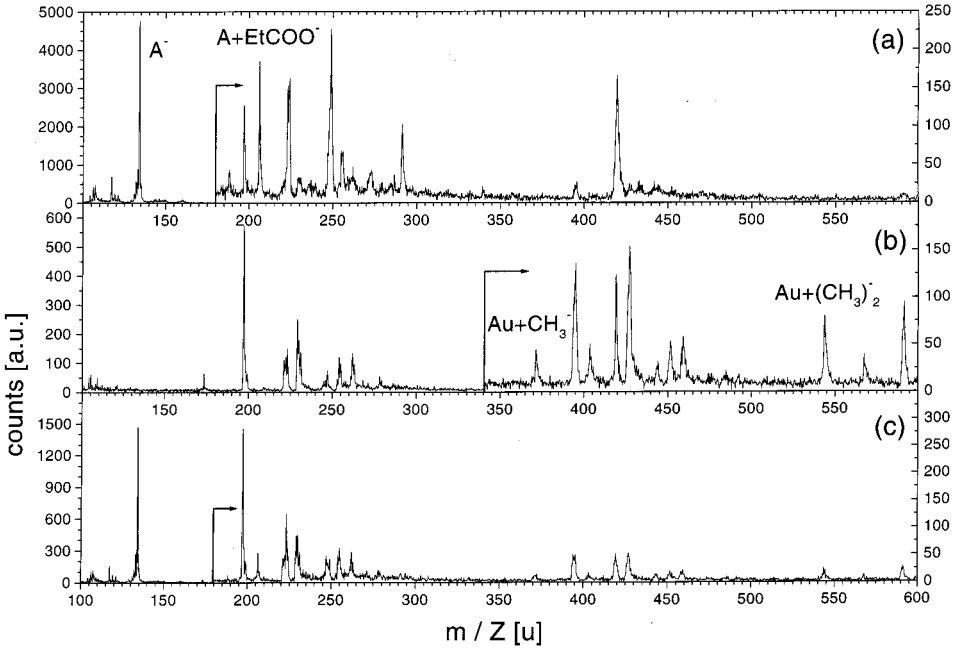

Figure 4. SDMS spectra of (a) a pure adenine thiolate SAM, (b) a pure CH_3T SAM, and (c) a SAM self-assembled out of a 19:2 (adenine/CH_3T) binary solution on gold.

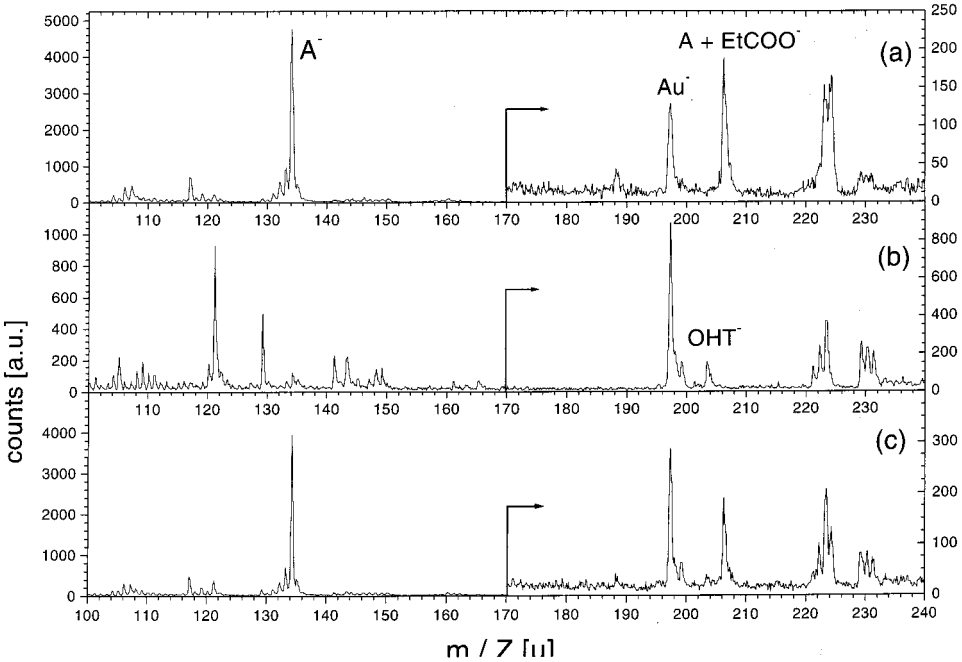

Figure 5. SDMS spectra of (a) a pure adenine thiolate SAM, (b) a pure OHT SAM, and (c) a SAM self-assembled out of a 19:2 (adenine/OHT) binary solution on gold.

A similar behavior is found by the contact angle measurements. Figure 7 depicts the advancing and receding contact angles of water on the CH_3T diluted adenine thiolate monolayers. High contact angles of around 100° representing hydrophobic surfaces are found for a wide mole fraction range of $x = 0$ to $x = 0.7$. For higher adenine concentrations the contact angles decrease steeply to 20−40° describing a hydrophilic surface. The hysteresis between advancing and receding contact angle shows the same behavior. For the high contact angle regime the hysteresis is small, about 10°, for the small contact angle regime the hysteresis is larger. At $x = 0.95$ a maximum of the hysteresis of 38° is found, which decreases for the pure adenine thiolate monolayer to 19°.

In Figure 8 the contact angle measurements for the OHT diluted adenine thiolate monolayers are shown. The development of the contact angles with increasing amount of adenine corresponds to the hydrophilic nature of the OH-termination. Starting at very low contact angles (5−12°) for the pure OHT at $x = 0$ the contact angles slightly increase up to $x = 0.82$ to 20−40°. The hysteresis is constant from $x = 0$ to $x = 0.82$ at around 7° and increases to 18° at $x = 0.95$. For the pure adenine thiolate monolayer the hysteresis reaches the maximum of 19°.

Multimode waveguide-PSP-coupling experiments were performed for adenine thiolate monolayers diluted with OHT only.[23] The average geometrical thicknesses and the average refractive indices of these mixed monolayers are depicted in Figure 9.

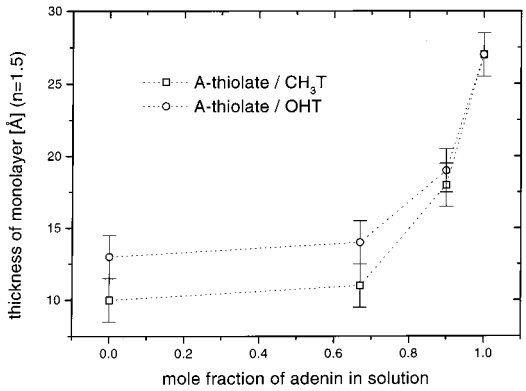

Figure 6. Thickness of the mixed monolayers ($n = 1.5$) versus mole fraction of the adenine in the self-assembly solution: for CH_3T (□) and OHT (○).

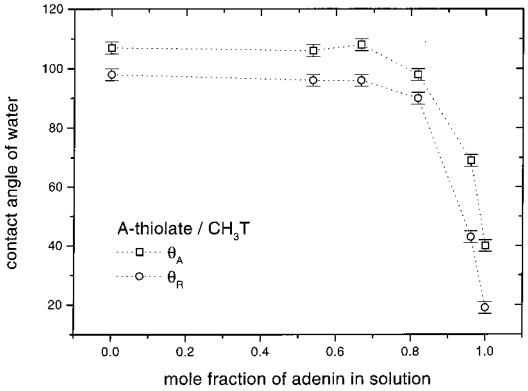

Figure 7. Advancing (□) and receding (○) contact angle of water versus the mole fraction of adenine in the self-assembly solution for CH_3T as the diluting molecule.

Both thickness and refractive index are only slowly increasing with increasing mole fraction of the adenine disulfide in solution. Both refractive index and film thickness are close to the values expected for pure OHT monolayers.[20] At very high mole fractions of adenine in solution the average geometrical thickness reaches 22 Å and a refractive index n of 1.53.

Discussion

The results from the electrochemical investigations show that self-assembled monolayers of OHT and adenine thiolate were formed on the gold surfaces. The smaller surface coverage of adenine thiolate compared to the OHT is considered to be caused by the larger headgroup of the adenine compound.

The thiols and the disulfides are covalentely bound to the gold surface as thiolates.[20] All the mass spectra depict the peak for the AuS^- ion and show specific peaks for the self-assembled monolayers for the pure ones as well as for the mixed ones.[44] The OHT and the CH_3T are able to dilute the adenine thiolate monolayers and exhibit the expected surface hydrophilicity or hydrophobicity. The PSP measurements yield thicknesses for the pure OHT and CH_3T which are in perfect agreement with the literature.[45] The model of the parallel aligned alkyl chains with a tilt angle of 25−30° to the surface normal can be applied.

An analogue construction of the monolayer for the adenine thiolate taking into account the geometry of the purine ring[46] leads to a thickness of 29 Å. For the PSP data analysis with a refractive index of 1.5 a layer thickness of 28 Å was found

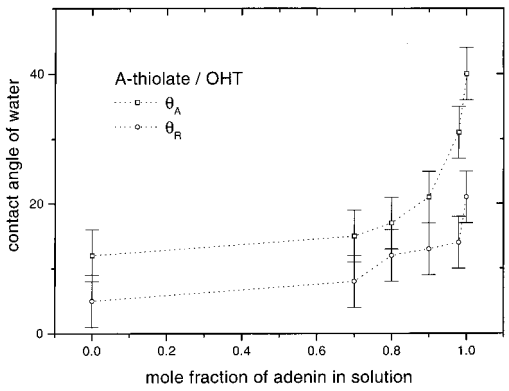

Figure 8. Advancing (□) and receding (○) contact angle of water versus the mole fraction of adenine in the self-assembly solution for OHT as the diluting molecule.

which is reasonable. However, the area per molecule value of 31 ± 3 Å^2 or 26 ± 3 Å^2, from the electrochemical measurements, respectively, yields a much higher surface density than that calculated for a stretched molecular arrangement with an area per molecule of 36 Å^2.[47] The large hysteresis of the contact angle measurements for the pure adenine thiolate monolayers points to a rough surface, caused by an unorganized film. A modified monolayer architecture has therefore to be taken into account. Obviously more adenine thiolates are bound to the surface than adenine headgroups could be exposed to the surface. A theoretical investigation has shown for cyclodextrin thiols, molecules with a similar geometry, that they can form monolayers consisting of molecules which are stretched and which expose the active group and in addition molecules which are filling the space under and between the stretched species.[38] The measured high refractive index of the pure adenine thiolate film also supports the filling of the space under the large adenine groups. If the density of the grafted molecules would be influenced only by the tight packing of the headgroups, the overall refractive index must be lower, because of the smaller density of the film under the adenine.

This behavior is one of the two distinct differences between the two-dimensional arrangements of adenine-containing amphiphiles at the air−water interface on LB troughs and adenine thiolates self-assembled on a metal. In the case of the air−water interface the molecules are arranged with respect to the size of their headgroups, whereas in the case of the self-assembly approach the grafting density is dominated by the binding of the much smaller thiolate groups. Therefore, it is necessary to dilute the active molecules of the self-assembled monolayer with proper inactive molecules. The concentration of the active species within the self-assembled monolayer, the adenine thiolate, respectively, then does not necessarily have to be identical with the concentration in the self-assembly solution. This seems to be the case with both of the chosen diluting molecules. All measurements point to a concentration behavior of the adenine thiolate on the surface which is strongly shifted to very high adenine concentrations within the self-assembly solution. Either the thickness, as the contact angles and their hysteresis show an influence of the adenine thiolate content in the self-assembled monolayers first from solution mole fractions of $x \geq 0.8$. Therefore the mass spectra were analyzed in a quantitative way. First of all the number of counts within a molecular specific peak are integrated for the pure monolayers. For the pure adenine thiolate monolayer the deprotonated adenine peak at $m/z = 134$ u and the deprotonated carboxy-

(45) Ulmann, A. *Ultrathin organic films*; Academic Press: Boston, 1991.
(46) Solomons, T. W. G. *Organic Chemistry*; Wiley & Sons: New York, 1994.
(47) Boland, T.; Ratner, B. D. *Langmuir* **1994**, *10*, 3845.

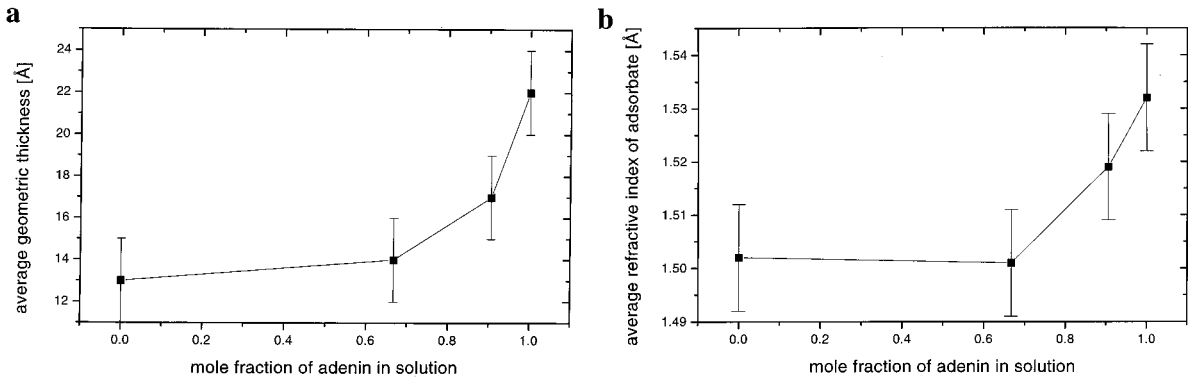

Figure 9. (a) Average geometrical thickness and (b) average refractive index of the adenine thiolate/OHT mixed monolayers versus mole fraction of adenine in solution.

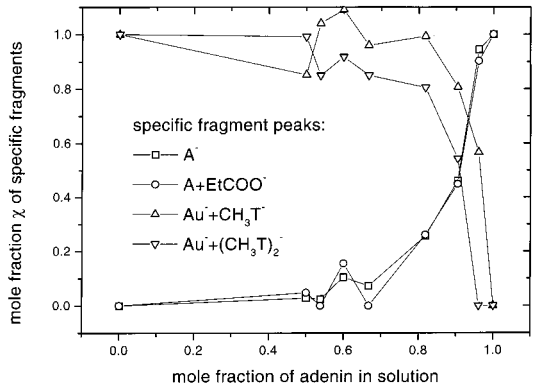

Figure 10. Mole fraction χ in the monolayer of two specific fragments of the adenine thiolate, namely A^- (-□-) and $A+EtCOO^-$ (-○-) and two specific fragments of CH_3T, namely, $Au + CH_3T^-$ (-△-) and $Au + (CH_3T)_2^-$ (-▽-), of the mixed self-assembled monolayer versus the mole fraction of adenine in the self-assembly solution.

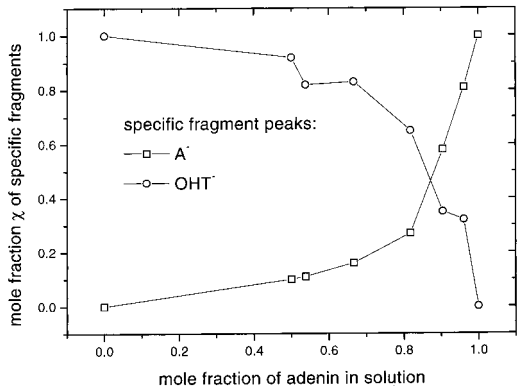

Figure 11. Mole fraction χ in the monolayer of a specific fragment of the adenine thiolate, namely, A^- (-□-), and a specific fragment of OHT, namely, OHT^- (-○-), of the mixed self-assembled monolayer versus the mole fraction of adenine in the self-assembly solution.

ethyladenine peak at $m/z = 206$ u were taken into account. The CH_3T monolayer is characterized by the specific peaks of the decanthiol ion at $m/z = 173$ u, the gold thiolate ion at $m/z = 370$ u and the gold didecan thiolate at $m/z = 543$ u. For the OHT monolayer only the peak at $m/z = 203$ u, the deprotonated mercaptoundecanal ion. The integrals over these peaks $I_{P100\%}$ are normalized by the total counts of that particular mass spectrum $I_{T100\%}$. The value $I_{P100\%}/I_{T100\%}$ corresponds to a mole fraction of 1: a gold surface which is covered by one thiolate species only. For the mixed monolayers the specific peaks $I_{Px\%}$ in the mass spectra are also integrated and normalized by the number of counts of the total spectrum $I_{Tx\%}$. The mole fraction χ of the fragment, and therefore of the thiolate under investigation in the monolayer is

$$\chi = \frac{I_{Px\%}/I_{Tx\%}}{I_{P100\%}/I_{T100\%}} \qquad (2)$$

The mole fractions χ calculated by eq 2 for the adenine thiolate−CH_3T mixed monolayer for four specific fragment peaks of both molecular species versus the mole fraction x of the adenine in solution are shown in Figure 10. For mole fractions of the adenine in solution from $x = 0$ to $x = 0.8$ specific fragments ($Au + CH_3T^-$ and $Au + (CH_3T)_2^-$) with a mole fraction χ on the gold surface of 0.8−1 are found for the CH_3T. The mole fractions of the adenine thiolate specific fragments (A^- and $A + EtCOO^-$) on the gold surface are increasing slowly to a mole fraction χ of maximal 0.25 at $x = 0.82$. From $x = 0.82$ to $x = 1$ the mole fraction χ of the adenine thiolate fragments on the gold increases to 1, while at the same time the mole fraction of the diluting molecule decreases. The sum of the mole fractions of the adenine thiolate and the CH_3T are close to 1 within the experimental errors. A 1/1 mixed monolayer on the gold can be self-assembled out of an adenine disulfide solution containing 90% adenine.

A similar picture is found for the OHT−adenine thiolate mixed monolayers. The results from the mass spectra data analysis via eq 2 are seen in Figure 11. Also in this case the specific fragment for the diluting molecule OHT shows up with a mole fraction χ of 1−0.8 on the gold surface between adenine concentrations in solution from $x = 0$ to $x = 0.7$. From $x = 0.7$ to the pure adenine disulfide solution the mole fraction χ of the adenine thiolate on the gold surface increases from 0.2 to 1. The 1/1 mixed monolayer can be achieved by self-assembling in an 85% adenine solution. The sum of the mole fractions χ of both fragments on the gold surface is one within the experimental errors.

Both diagrams clearly depict that the concentrations within the self-assembly solution and on the gold surface are not identical. A very high mole fraction of the adenine disulfide in solution is necessary to find adenine thiolates on the gold surface. This behavior can be explained by the intermolecular interactions. It is known, that the van der Waals interaction between the alkyl chains in self-assembled monolayers gives a major enthalpic contribution to the order and structure. Estimations show that per CH_2 group a cohesive energy of 6.9 kJ/mol are expected.[39−41,45,48−51] In the pure adenine thiolate monolayer

(48) Israelachvili, J. N. *Intermolecular and surface forces*; Academic Press: London 1992.
(49) Pertsin, A. J.; Grunze, M. *Langmuir* **1994**, *10*, 3668.
(50) Whitesides, G. M.; Laibinis, P. E. *Langmuir* **1990**, *6*, 87.

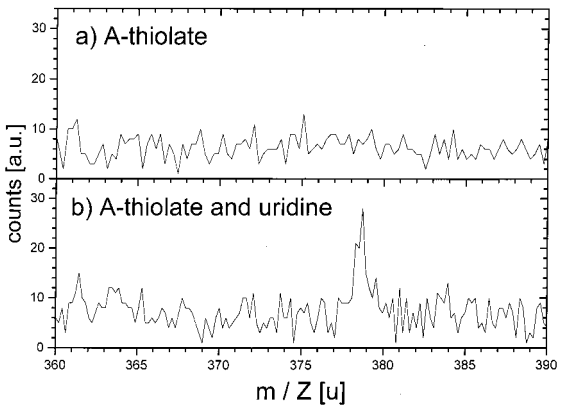

Figure 12. SDMS spectra of pure adenine thiolate SAM (a) without and (b) with uridine immersion.

the steric hindrance of the adenine headgroups prevent an optimal packing. Every added diluting molecule (CH_3T or OHT) will bring an enormous enthalpic contribution (ca. 60kJ/mol) to the monolayer by interdigitating with the adenine thiolates.[39−41,45,48,49] This process will promote the build in of diluting molecules until an average area per molecule of 36 Å^2, the needed space for an adenine thiolate, is reached. This surface density can be achieved at a mixing ratio of 1:1 on the surface.

The results from the multimode waveguide-PSP-coupling experiments fit perfectly within this picture. The average geometrical thickness only increases when adenine thiolate is built into the monolayer at high adenine disulfide concentrations in solution. Then the thickness reaches a value of 22 Å which is smaller than the comparable value of 28 Å calculated from the surface plasmon measurements. The behavior for the refractive index is pretty similar. As long as the OHT is the dominant feature within the monolayer a refractive index n of 1.5 fits the data very well. At the high adenine thiolate concentrations the average refractive index increases to 1.53. This refractive index is an average over the alkylchain with $n = 1.5$ and the conjugated adenine headgroup. Therefore, by estimating a refractive index of 1.5 for the complete molecule leads to a too high monolayer thickness (PSP).

Base Pairing

Measurements. For the base pairing self-assembled monolayers of all pure species and of various mixtures were prepared. The specific and unspecific reaction of uridine as well as the unspecific reaction of cytidine were tested. The mass spectrum taken from a pure adenine thiolate monolayer which was rinsed with a uracil solution shows an additional mass peak at $m/z = 378$ u compared to the mass spectrum of the pure adenine thiolate monolayer (Figure 12). This mass represents the deprotonated complex of adenine and uridine. The pure adenine thiolate monolayer which was rinsed with a cytidine solution does not show a corresponding peak of an adenine complexed with the cytosine. A binding of cytosine could also not be detected in any mass spectra of adenine containing monolayers rinsed with cytosine, neither mixed with CH_3T nor with OHT.

The mass spectra of the mixed monolayers of adenine thiolate and CH_3T or OHT are different from each other with respect to the mass peak at $m/z = 378$ u. The mixed monolayers of adenine thiolate and OHT show even for very low adenine concentrations within the monolayer a distinct adenine−uridine complex peak. Nevertheless, the intensities of the peaks are too low for a data analysis via eq 2 to quantify the amount of uridine. The binary mixed monolayers of adenine thiolate and CH_3T do not show the peak of the complexed base pair, independently on the concentration of the adenine in the monolayer.

Also with respect to the fragments of the uridine with $m/z = 111$ and 243 u the monolayers show clear differences. Pure adenine thiolate monolayers and binary mixtures with OHT that were rinsed with uridine depict both of these mass peaks in the mass spectra, whereas mass spectra of binary mixtures of adenine thiolate and CH_3T, as well as those of the pure monolayers of OHT and CH_3T all rinsed in uridine solution, do not show any of these mass peaks.

The adsorption kinetics of uridine and cytosine were followed for a pure gold surface and a series of pure and mixed monolayers with PSP spectroscopy. At a given time the water in the cuvette is exchanged by a uridine- or cytidine-containing solution. After about half an hour the cuvette is rinsed again with pure water. During the rinsing a part of the adsorbed molecules is removed. The thickness results of these kinetic are summarized in Table 3. The thickness after the adsorption process and the thickness after the rinsing with pure water after the adsorption are chosen. Both nucleotides show a strong adsorption to pure gold surfaces. Thicknesses of up to 9 Å for cytosine were found. In the overall comparison cytosine seems to adsorb stronger to any surface than uridine. For all monolayers the thickness of the adsorbed cytosine layer is larger than that for the adsorbed uridine layer, with one exception: for the OHT-diluted adenine thiolate monolayer the adsorbed uridine shows a higher thickness.

Adsorption measurements of uracil and cytosine on adenine thiolate/OHT mixed monolayers with $x = 0.9$ performed with the multimode waveguide-PSP-coupling technique yielded a thickness of 6 ± 2 Å and a refractive index of $n = 1.53 \pm 0.01$ for uracil. The test for unspecific binding with cytosine leads to a signal which is not significant within the noise of the experiment.

Table 3. Thickness of the Adsorbed Uridine or Cytosine Layer, Respectively, Measured by Surface Plasmon Kinetic Scans before and after Rinsing with Pure Water after 30 min of Adsorption Time[a]

	uridine layer thickness [Å]		cytidine layer thickness [Å]	
	before rinsing	after rinsing	before rinsing	after rinsing
pure gold surface	6	3	9	6
pure adenine thiolate	5	3	7	4
pure OHT	3	1	6	3
pure CH_3T	2	1	4	2
adenine thiolate/OHT	7	5	5	2
adenine thiolate/CH_3T	3	1	-	-

[a] The error is ±1.5 Å. For the mixed monolayers of adenine thiolate and OHT or CH_3T a mole fraction of $x = 0.9$ was chosen.

Discussion

The central question, whether the uridine binds specifically to the two-dimensional assembled adenine, can clearly be answered with yes. The presence of the peak in the mass spectra of the uridine−adenine complex can only exist when uridine is binding specifically to the adenine at this water−solid interface. The PSP and multimode waveguide-PSP-coupling technique data confirm the base-pair reaction. The film thickness of bound uracil after rinsing is higher than the thickness of the adsorbed cytosine in the case of the $x = 0.85$ adenine thiolate/OHT monolayer. Nevertheless, there is big tendency for unspecific

(51) Strong, L.; Whitesides, G. M. *Langmuir* **1988**, *4*, 546.

binding both for uridine and cytosine. On all samples under investigation (Table 3) both nucleotides adsorb even at surfaces without any binding sites (gold, CH_3T, and OHT), but the mass never shows a peak due to a complex formed from adenine and cytosine. Thus, the cytosine adsorption must always be unspecific. Only in the case where an optimal adenine density within the monolayer is achieved ($x = 0.9$) can the uridine binding be considered to be specific. A dilution of the active adenine thiolate is necessary to achieve a proper binding. The adenine−uracil complex mass peak and the two other specific uracil fragments are indeed present for a pure adenine thiolate and an adenine thiolate/OHT monolayer, but the uracil thickness measured by PSP indicates a specific binding only for the optimized mixed adenine thiolate/OHT monolayer.

It is totally unclear why the mixed adenine thiolate/CH_3T monolayers do not show a binding. In the mass spectra no adenine−uracil complex or uracil fragments could be detected, and the PSP measurements show only very small thicknesses for uridine and no adsorption at all for cytosine at the mixed adenine thiolate/CH_3T monolayer. For the pure CH_3T monolayer unspecific binding is found mainly for cytidine. There might be an interaction between the hydrophobic headgroups of the CH_3T and the adenine heads in the active thiolate which hinder the adsorption of the uracil.

The measured refractive index for uracil is higher than usually estimated. The nucleosides consist of conjugated units and therefore have a higher polarizability compared to alkyl chains leading to an enhanced refractive index.

Conclusions

We have shown the preparation and characterization of immobilized monolayers containing adenine in a two-dimensional geometry as a solid−water interface. Via self-assembly of disulfides and thiols onto gold out of pure or binary mixed solutions the adenine content within the adenine-containing monolayer could be adjusted. The specific base-pair reaction between this two-dimensional immobilized adenine and uracil could be shown by mass spectroscopy and optical methods. Unspecific binding both of uracil and cytosine was found, too. This unspecific binding can lead to problems, if such a system is used in a sensor device.

JA990447B